Journal of Nuclear Materials 389 (2009) 164–169

Contents lists available at ScienceDirect

Journal of Nuclear Materials

journal homepage: www.elsevier.com/locate/jnucmat

Analysis of oxygen potential of $(U_{0.7}Pu_{0.3})O_{2\pm x}$ and $(U_{0.8}Pu_{0.2})O_{2\pm x}$ based on point defect chemistry

Masato Kato [a,*], Kenji Konashi [b], Nobuo Nakae [a,c]

[a] Japan Atomic Energy Agency, Tokai-mura, 4-33 Muramatsu Naka-gun, Ibaraki 319-1194, Japan
[b] Tohoku University, 2145-2, Narita, Oarai-machi, Ibaraki 311-1313, Japan
[c] Japan Nuclear Energy Safety Organization, TOKYU REIT Toranomon Bldg, 3-17-1, Toranomon, Minato-ku, Tokyo 105-0001, Japan

A B S T R A C T

Stoichiometries in $(U_{0.7}Pu_{0.3})O_{2\pm x}$ and $(U_{0.8}Pu_{0.2})O_{2\pm x}$ were analyzed with the experimental data of oxygen potential based on point defect chemistry. The relationship between the deviation x of stoichiometric composition and the oxygen partial pressure P_{O_2} was evaluated using a Kröger–Vink diagram. The concentrations of the point defects in uranium and plutonium mixed oxide (MOX) were estimated from the measurement data of oxygen potentials as functions of temperature and P_{O_2}. The analysis results showed that x was proportional to $P_{O_2}^{\pm 1/2}$ near the stoichiometric region of both $(U_{0.7}Pu_{0.3})O_{2\pm x}$ and $(U_{0.8}Pu_{0.2})O_{2\pm x}$, which suggested that intrinsic ionization was the dominant defect. A model to calculate oxygen potential was derived and it represented the experimental data accurately. Further, the model estimated the thermodynamic data, $\Delta\overline{H}_{O_2}$ and $\Delta\overline{S}_{O_2}$, of stoichiometric $(U_{0.7}Pu_{0.3})O_{2.00}$ and $(U_{0.8}Pu_{0.2})O_{2.00}$ as -552.5 kJ·mol^{-1} and -149.7 J·mol^{-1}, and -674.0 kJ · mol^{-1} and -219.4 J · mol^{-1}, respectively.

1. Introduction

Uranium and plutonium mixed oxide (MOX) having fluorite structure has been used as fuels in fast reactors [1,2]. It is well-known that this mixed oxide is an oxygen non-stoichiometric compound which is stable in hyper- and hypo-stoichiometric compositions [3,4]. The stoichiometry strongly affects oxide physical properties, thermal conductivities, diffusion coefficients, lattice parameters, oxygen potentials and so on [4–8]. Therefore, many studies on oxygen potentials have been carried out as parameters of Pu content, temperature and oxygen-to-metal ratio (O/M), and some models to represent oxygen potentials were derived [9–14].

Non-stoichiometry of oxides has been analyzed by a point-defect scheme using experimental oxygen potentials. Recently Karen [15] methodically outlined a point-defect scheme for description of non-stoichiometry in extended structures of oxides, and he calculated oxygen-content using experimental data. Sasaki and Maeir [16] numerically calculated defect concentration and estimated standard enthalpy and mass action constant. Some studies were also carried out for actinide oxides [17,18]. Nakamura and Fujino [14] represented non-stoichiometry in UO_{2+x} by a point-defect model and suggested the need for further experimental work to better assess the model.

Oxygen potential measurements of MOX have been carried out by many researchers. The data, however, are scattered with an error of more than ±100 kJ · mol^{-1} in the near stoichiometric region. In previous works, Kato et al. [19,20] measured oxygen potentials of $(U_{0.7}Pu_{0.3})O_{2-x}$ and $(U_{0.8}Pu_{0.2})O_{2-x}$ in the near stoichiometric region by a gas equilibrium method. The data were obtained with high repeatability, and the relation between their stoichiometry and oxygen partial pressure was discussed. The aim of the present work is to analyze point defect concentration in MOX and to obtain a quantitative model which represents the oxygen potentials of MOX as functions of oxygen non-stoichiometry and temperatures using the reported data.

2. Data sources used in the analysis

2.1. Oxygen potential data for hypo-stoichiometric MO_{2-x}

The oxygen potentials were measured for MOX having a variety of stoichiometries at various temperatures by different methods. In the present work, the oxygen potentials of MOX containing 20% and 30% Pu were analyzed and discussed. The details of data sources which used in this analysis are shown in Table 1. Vasudeva Rao et al. [21] also reported oxygen potentials of MOX containing 20% and 31% Pu. They measured those data by using a furnace, and the O/M ratio was decided after the measurement. Such experiment is not certain whether a sample does or does not attain equilibrium condition. In addition, variations of oxygen potential during heating and cooling process may cause larger error. Therefore, their data were not used for this analysis.

* Corresponding author. Tel.: +81 29 282 1111; fax: +81 29 282 9473.
E-mail address: kato.masato@jaea.go.jp (M. Kato).

0022-3115/$ - see front matter © 2009 Elsevier B.V. All rights reserved.
doi:10.1016/j.jnucmat.2009.01.023

Table 1
Data sources of oxygen potentials of MOX used in this work.

	Method	Pu content (%)	O/M range	Temperature range (K)	Number of points
Markin and McIver[22]	EMF[a]	11	2.000–2.077	1073–1373	20
Chilton and Kirkham[25]	TG[b]	15	2.002–2.106	1518–1823	24
Javed [26]	TG[c]	20	1.920–1.989	1273–1973	20
Kato et al.[20]	TG[c]	20	1.9911–2.0000	1473–1623	66
Markin and McIver[22]	EMF[a]	30	1.868–2.062	1073–1373	39
Chilton and Edwards[24]	TG [b]	31	1.994 - 2.074	1244-1823	52
Kato et al.[19]	TG [c]	30	1.9700–2.0000	1273–1623	81

[a] Electromotive force method.
[b] Thermal gravimetry using CO_2/CO gas mixture.
[c] Thermal gravimetry using H_2O/H_2 gas mixture.

The oxygen potential data for hypo-stoichiometric MOX containing about 30% Pu content was obtained and reported by several groups [19, 22–25]. Fig. 1 shows the deviation x from stoichiometry plotted against oxygen partial pressure (P_{O_2}) [19]. As shown in this figure, the relationship between x and P_{O_2} with a fixed temperature is expressed by two lines having different slopes. It is well known that the slope should correspond to point defects introduced in non-stoichiometric oxides [14, 17–20]. The following relationship should be generally obtained

$$x \propto P_{O_2}^{1/n},$$

where n is a characteristic number identifying the type of point defects and it corresponds to the slope. Fig. 1 indicates that n equals -2 in the near stoichiometric region and changes to -3 with increasing x. The changes of n and/or slope should suggest that the type of lattice defects changes with increasing lattice defect concentration. The lattice defect structure is discussed in the next section.

The data of $(U_{0.8}Pu_{0.2})O_{2-x}$ were measured by Kato et al. [20] and Javed [26], and Kato et al. reported them as Fig. 2. Other researchers [18, 24, 25] also reported data for $(U_{0.8}Pu_{0.2})O_{2-x}$, but their data were significantly higher as compared with other measured data [20, 26] and the calculated data [20] represented by Bessmen and Lindmer's model. Therefore the two data sets which were measured by Kato et al. [20] and Javed [26] were used to analyze the oxygen potential of $(U_{0.8}Pu_{0.2})O_{2-x}$ in this work. Fig. 2 shows that n equals -2 in the near stoichiometric region and changes to -4 with increasing x. As shown Figs. 1 and 2, the relationship is $n = -2$ in the near stoichiometric region of both samples, $(U_{0.7}Pu_{0.3})O_{2-x}$ and $(U_{0.8}Pu_{0.2})O_{2-x}$, and then n changes to different values of $n = -3$ and -4, respectively, with increasing x. This difference suggests that different types of point defects dominate in each sample.

2.2. Oxygen potential data for hyper-stoichiometric MO_{2+x}

The oxygen potential data for hyper-stoichiometric MOX containing about 30% Pu content were reported by several groups [22–25]. The data are plotted in Fig. 3 in the same manner as in Fig 1. The scattering of the data increased with decreasing x, which was due to the measurement error of thermal gravimetry. It is considered that the variation in the region of $x \leqslant 10^{-3}$ is unreliable because of the greater scattering. As shown in Fig. 3, the relationship between x and P_{O_2} with a fixed temperature is expressed by only one line, and n equals +2.

The data of $(U_{0.85}Pu_{0.15})O_{2+x}$ and $(U_{0.89}Pu_{0.11})O_{2+x}$ are plotted in Fig. 4. Both have the same relationship of $n = +2$ as well as the same variation seen for $(U_{0.7}Pu_{0.3})O_{2+x}$. It is expected that the relationship for $(U_{0.8}Pu_{0.2})O_{2+x}$ is also $n = +2$, although data for $(U_{0.8}Pu_{0.2})O_{2+x}$ have not been reported yet. Kofstad [17] reported that the value of n was +2 in UO_{2+x} having O/M ratio from 2.00 to 2.10. The relationship in hyper-stoichiometric MOX was the same as that of UO_{2+x}.

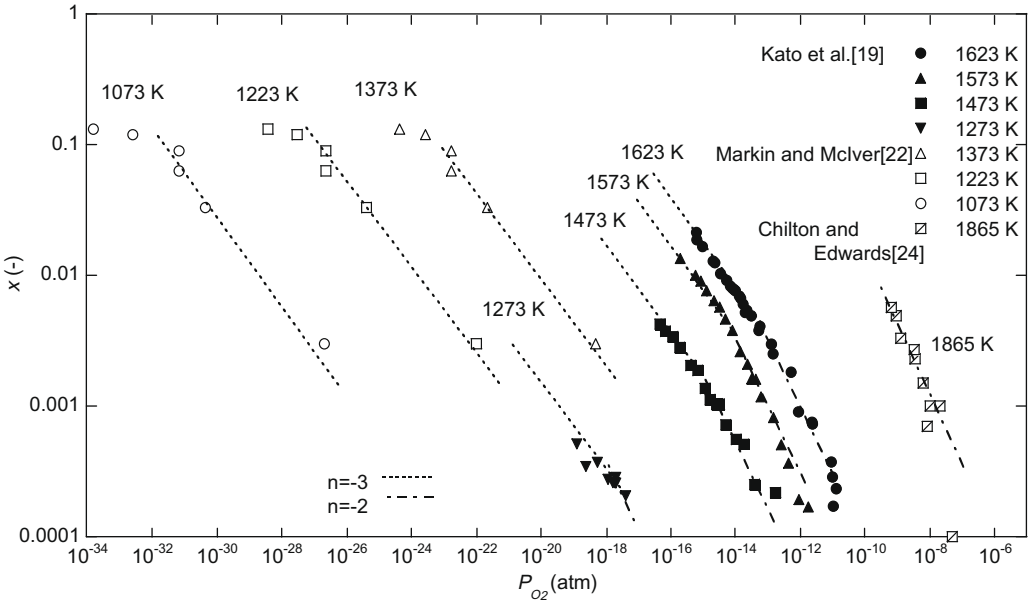

Fig. 1. The relationship between x and P_{O_2} in $(U_{0.7}Pu_{0.3})O_{2-x}$ [19].

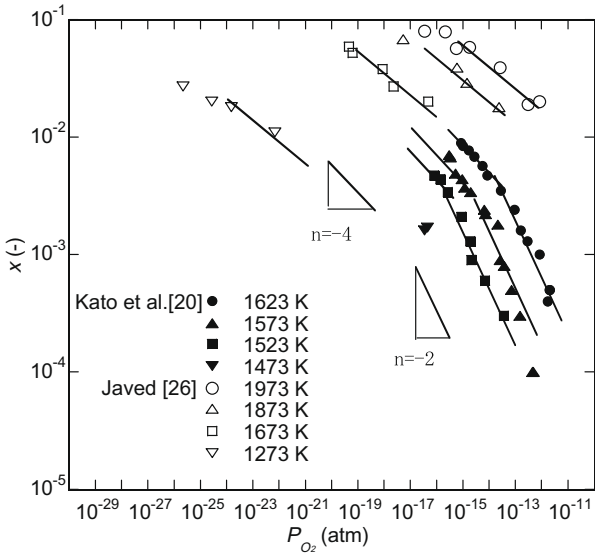

Fig. 2. The relationship between x and P_{O_2} in $(U_{0.8}Pu_{0.2})O_{2-x}$ [20].

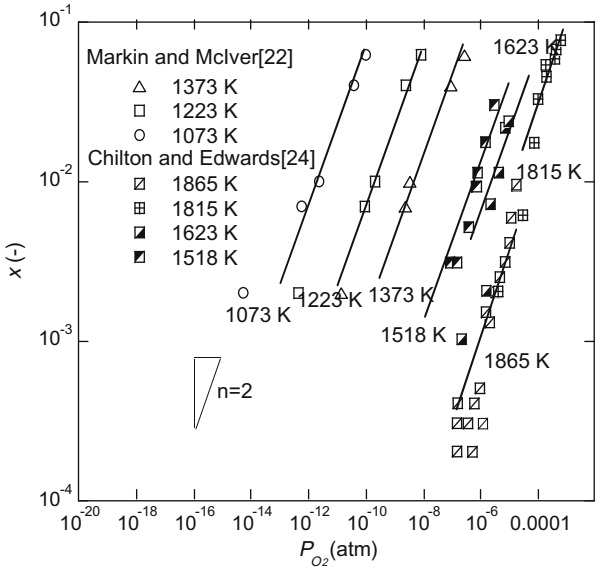

Fig. 3. The relationship between x and P_{O_2} in $(U_{0.7}Pu_{0.3})O_{2+x}$.

3. Results and discussion

Brouwer [27] and Kröger and Vink [28] evaluated the relationship between defect concentrations and oxygen partial pressure in various non-stoichiometric compounds. This work also evaluated the oxygen potential of the mixed oxides by their analytical method and the Kröger–Vink [28] notation is used here.

Some types of point defects have been reported in MOX. The defect cluster of $(Pu'V_O^{\cdot\cdot}Pu')$ was proposed in hypo-stoichiometric compounds [29–31]. Beauvy [32] reported that the defect clusters of $(Pu'V_O^{\cdot\cdot}Pu')$ and $(Pu'V_O^{\cdot\cdot}Pu^{\times})$ and those of $(Pu'V_O^{\cdot\cdot}U')$ and $(Pu'V_O^{\cdot\cdot})$ were stable in compounds with more than and less than 15 at% plutonium, respectively.

In the region of low oxygen partial pressure, $(U_{0.7}Pu_{0.3})O_{2-x}$ has the relation of $n = -3$ as shown in Fig. 1. However no point defect having $n = -3$ has been reported in MOX. Here, the following defect is assumed to fit $n = -3$.

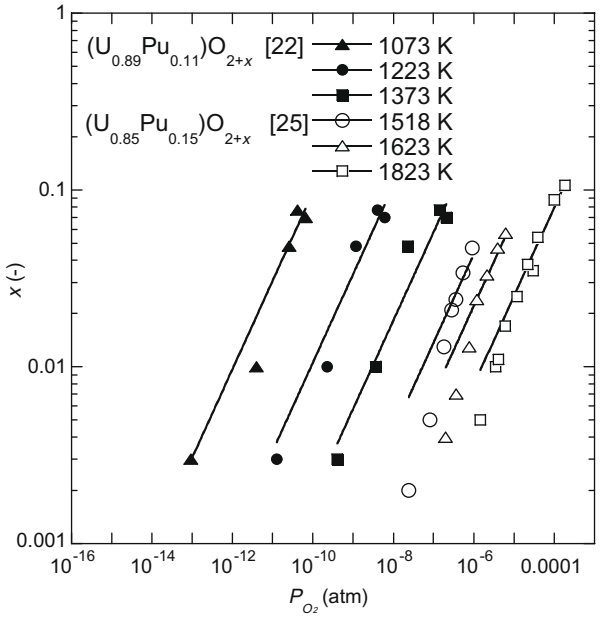

Fig. 4. The relationship between x and P_{O_2} in $(U_{0.89}Pu_{0.11})O_{2+x}$ and $(U_{0.85}Pu_{0.15})O_{2+x}$.

$$2O_O^{\times} + 2Pu_{Pu}^{\times} \rightarrow (2V_O^{\cdot\cdot}2Pu')^{\cdot\cdot} + 2e' + O_2 \quad (1)$$

On the other hand, $n = +2$ at the high oxygen pressure as shown in Fig. 3. In this region the defect of a 2:2:2 cluster is assumed, the same as that in UO_{2+x}, and the defect reaction is as follows [33]:

$$2O_O^{\times} + O_2 \rightarrow (2O_i^a 2O_i^b 2V_O)' + h^{\cdot} \quad (2)$$

In addition, the following reactions are considered for structural defects.

$$Nill \rightarrow e' + h^{\cdot} \quad (3)$$

$$O_O^{\times} \rightarrow V_O^{\cdot\cdot} + O_i'' \quad (4)$$

$$O_O^{\times} \rightarrow V_O^{\cdot\cdot} + 2e'_{Pu} + \frac{1}{2}O_2 \quad (5)$$

$$O_O^{\times} \rightarrow O_i'' + h^{\cdot} \quad (6)$$

The equilibrium constants, K_{Re}, K_{Ox}, K_i, K_F, K_{V_O} and K_{Oi_O} in the defect reactions (1)–(6), are described as Eqs. (7)–(12), respectively

$$K_{\mathrm{Re}} = [(2V_O^{\cdot\cdot}2Pu')^{\cdot\cdot}][e']^2 P_{O_2} \quad (7)$$

$$K_{Ox} = [(2O_i^a 2O_i^b 2V_O)'][h^{\cdot}]P_{O_2}^{-1} \quad (8)$$

$$K_i = [h^{\cdot}][e'] \quad (9)$$

$$K_F = [V_O^{\cdot\cdot}][O_i''] \quad (10)$$

$$K_{V_O} = [V_O^{\cdot\cdot}][e']^2 P_{O_2}^{1/2} \quad (11)$$

$$K_{Oi_O} = [O_i'')[h^{\cdot}]P_{O_2}^{-1/2} \quad (12)$$

Two cases are considered in the near stoichiometric region, which are dominated by intrinsic ionization and Frenkel defects as shown in Eqs. 3 and 4, respectively [17,18]. When the Frenkel defect is the dominant defect for the near stoichiometric composition, the deviation x is null because $[V_O^{\cdot\cdot}]$ is equal to $[O_i'']$. However the relation between x and P_{O_2} is $n = \pm 2$ in MOX as shown in Figs. 1 and 3 and that suggests that intrinsic ionization is the dominant defect in the region. Naito et al. [34] and Fujino et al. [35] measured the electrical conductivity of MOX and reported that the generation of electrons and holes was more important than generation of Frenckel defects near stoichiometry. It was reported that the defects in UO_2 were also dominated by intrinsic ionization [17]. These

observations are consistent, and show that intrinsic ionization is the dominant defect in stoichiometric MOX. Then, the reducing condition and oxidizing condition were evaluated as follows.

Region I: Near stoichiometric condition

In this region, $[h^{\cdot}]$ is equal to $[e']$ assuming that intrinsic ionization is dominant, and Eq. (9) can be written as

$$[h^{\cdot}] = [e'] = K_i^{1/2} \tag{13}$$

When inserting Eq. (13) into Eqs. 11 and 12, $[V_O^{\cdot\cdot}]$ and $[O_i'']$ are given by

$$[V_O^{\cdot\cdot}] = \frac{K_{V_O}}{[e']^2} P_{O_2}^{-1/2} = \frac{K_{V_O}}{K_i} P_{O_2}^{-1/2} \tag{14}$$

$$[O_i''] = \frac{K_{O_i}}{[h^{\cdot}]^2} P_{O_2}^{1/2} = \frac{K_{O_i}}{K_i} P_{O_2}^{1/2} \tag{15}$$

If the deviation x is given by

$$x = |\,([V_O^{\cdot\cdot}] - [O_i'])\,|,$$

the value of n becomes ±2 in the near stoichimetric region, which is consistent with the relationship shown in Figs. 1 and 3.

Region II: Reducing condition

In the defect reaction of Eq. (1), the electro-neutrality condition is given by

$$2[(2V_O^{\cdot\cdot}2Pu')^{\cdot\cdot}] = [e']$$

When inserting into Eq. (7), and the equilibrium constants, K_{Re}, is described as the following equation.

$$K_{\mathrm{Re}} = 4[(2V_O^{\cdot\cdot}2Pu')^{\cdot\cdot}]^3 P_{O_2}$$

$[V_O^{\cdot\cdot}]$ can be written as

$$[V_O^{\cdot\cdot}] = 2[(2V_O^{\cdot\cdot}2Pu')^{\cdot\cdot}] = (2K_{\mathrm{Re}})^{1/3} P_{O_2}^{-1/3} \tag{16}$$

The relation between oxygen pressure and x is derived as $n = -3$.

Region III: Oxidizing condition

In the defect reaction of Eq. (2), the electro-neutrality condition is given by

$$[(2O_i^a 2O_i^b 2V_O)'] = [h^{\cdot}]$$

When inserting into Eq. (8), and the equilibrium constants, K_{Ox}, is described as the following equation.

$$K_{Ox} = [(2O_i^a 2O_i^b 2V_O)']^2 P_{O_2}^{-1}$$

$$[O_i''] = 2[(2O_i^a 2O_i^b 2V_O)'] = 2K_{Ox}^{1/2} P_{O_2}^{1/2} \tag{17}$$

The data shown in Figs. 1 and 3 are fitted by Eqs. 14, 16, and 17 assuming that $x = [V_O^{\cdot\cdot}]$ and $x = [O_i'']$, and the equilibrium constants K_{Re}, K_{V_o}/K_i and K_{Ox} are estimated as a function of temperatures. The equilibrium constants are plotted in Fig. 5 and are given by Eqs. (18)–(22) as a function of temperature.

$$K_{\mathrm{Re}} = 2.033 \times 10^9 \exp(-930.4 \times 10^3/RT) \tag{18}$$

$$K' = K_{V_o}/K_i = 1104.1 \exp(-375.9 \times 10^3/RT) \tag{19}$$

$$K_{Ox} = 7.053 \times 10^{-11} \exp(353.2 \times 10^3/RT) \tag{20}$$

Assuming that Eqs. 18 and 19 are represented by the same line in Fig. 3, Eq. (23) is derived.

$$K'' = K_{O_i}/K_i = 2K_{Ox}^{1/2} \tag{21}$$

The oxygen-to-metal ratio is given by

$$O/M = 2 - [V_O^{\cdot\cdot}] + [O_i''] \tag{22}$$

The P_{O_2} values of $(U_{0.70}Pu_{0.3})O_{2\pm x}$ are represented as functions of O/M and temperature using Eqs. (14)–(22) and shown with experimental data in Fig. 6. The current model reproduces the experimental data very well.

The relation between oxygen potential ($\Delta\overline{G}_{O_2}$) and oxygen partial pressure (P_{O_2}) is written as

$$\Delta\overline{G}_{O_2} = RT \ln P_{O_2} \tag{23}$$

where R is the gas constant (8.314 J K^{-1} mol^{-1}) and T is absolute temperature.

It is important to estimate $\Delta\overline{G}_{O_2}$ at stoichiometric composition as exactly as possible because it has a strong influence on nuclear fuel behavior. When $[V_O^{\cdot\cdot}]$ is equal to $[O_i'']$, MOX has the stoichiometric composition. The $\Delta\overline{G}_{O_2}$ values of the stoichiometric MOX are calculated as a function of temperature and shown in Fig. 7 using Eqs. 14 and 15.

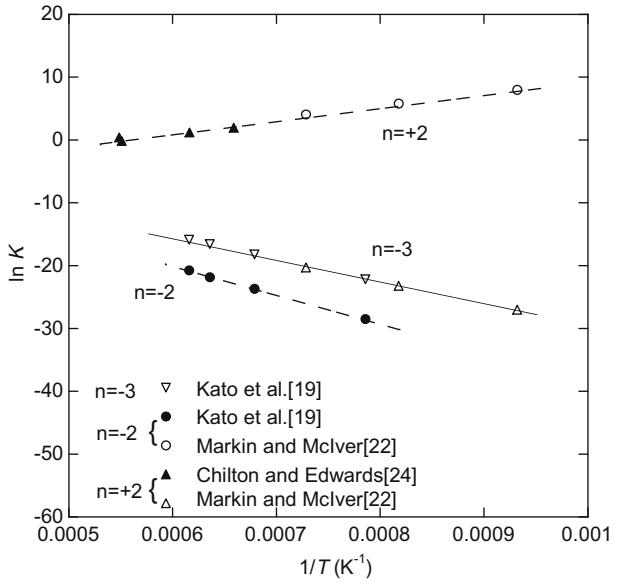

Fig. 5. ln K versus $1/T$.

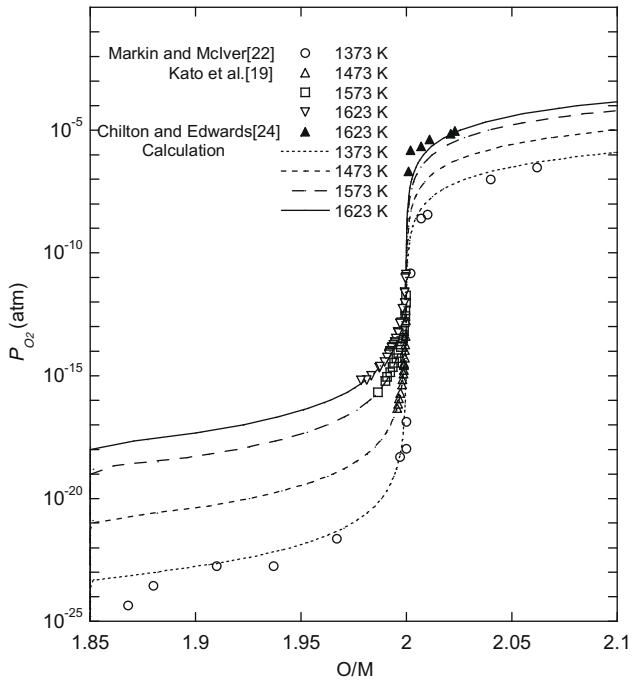

Fig. 6. Oxygen non-stoichiometry in $(U_{0.7}Pu_{0.3})O_{2\pm x}$ as a function of temperature and P_{O_2}.

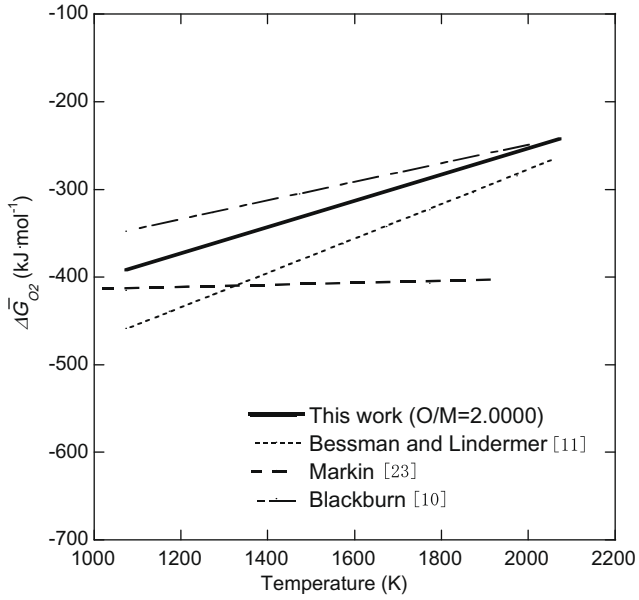

Fig. 7. The $\Delta\bar{G}_{O_2}$ of $(U_{0.7}Pu_{0.3})O_{2.00}$.

The calculated $\Delta\bar{G}_{O_2}$ values at stoichiometric composition are plotted as a function of temperature (T) together with those proposed by other workers [10, 11, 22] in Fig. 7. The $\Delta\bar{G}_{O_2}$ is given by the following relation,

$$\Delta\bar{G}_{O_2} = \Delta\bar{H}_{O_2} - T\cdot\Delta\bar{S}_{O_2}, \tag{24}$$

where $\Delta\bar{H}_{O_2}$ is partial molar enthalpy and $\Delta\bar{S}_{O_2}$ is partial molar entropy.

The trend obtained in the present work appears between the data calculated by two models [10, 11]. The $\Delta\bar{H}_{O_2}$ and $\Delta\bar{S}_{O_2}$ of $(U_{0.7}Pu_{0.3})O_{2.00}$ are estimated to be $-552.5\ \mathrm{kJ\cdot mol^{-1}}$ and $-149.7\ \mathrm{J\cdot mol^{-1}}$, respectively. It is considered that the current model gives better results than the other models in the near stoichiometric region, because the present model was derived from data measured recently in the near stoichiometric region.

The concentration of point defects in $(U_{0.8}Pu_{0.2})O_{2-x}$ is also analyzed. The relation between x and P_{O_2} is $n = -2$ in the near stoichiometric composition and varies to $n = -4$ with increasing x as shown in Fig. 2. The relation of $n = -4$ is different from that in $(U_{0.7}Pu_{0.3})O_{2-x}$. The defect reaction is assumed in this region is as follows:

$$O_O^{\times} + Pu_{Pu}^{\times} \rightarrow (V_O^{\cdot\cdot}Pu')^{\cdot} + e' + \frac{1}{2}O_2 \tag{25}$$

The K_{Re} can be written as

$$K_{\mathrm{Re}} = [(V_O^{\cdot\cdot}Pu')^{\cdot}][e']P_{O_2}^{1/2} \tag{26}$$

In other regions, the relation is analyzed by using the same defect reaction that is assumed in $(U_{0.7}Pu_{0.3})O_{2\pm x}$. The equilibrium constants of the defect reactions are given by

$$K_{\mathrm{Re}} = 5.81900\times10^{5}\exp(-541.7\times10^{3}/RT) \tag{27}$$

$$K' = K_{V_O}/K_i = 6.33\times10^{6}\exp(-497.8\times10^{3}/RT) \tag{28}$$

The K_{Ox} is estimated from experimental data for $(U_{0.89}Pu_{0.11})O_{2+x}$, $(U_{0.85}Pu_{0.15})O_{2+x}$ and $(U_{0.69}Pu_{0.31})O_{2+x}$, because no data have been obtained for $(U_{0.8}Pu_{0.2})O_{2+x}$, and the relations are same among their oxides as shown in Fig. 4. The K_{Ox} is given by

$$K_{Ox} = \exp(-8.105C - 21.22)\exp(353.2\times10^{3}/RT) \tag{29}$$

where C is Pu content. Fig. 8 shows P_{O_2} as functions of O/M and temperature in $(U_{0.8}Pu_{0.2})O_{2\pm x}$. The calculated results are in good

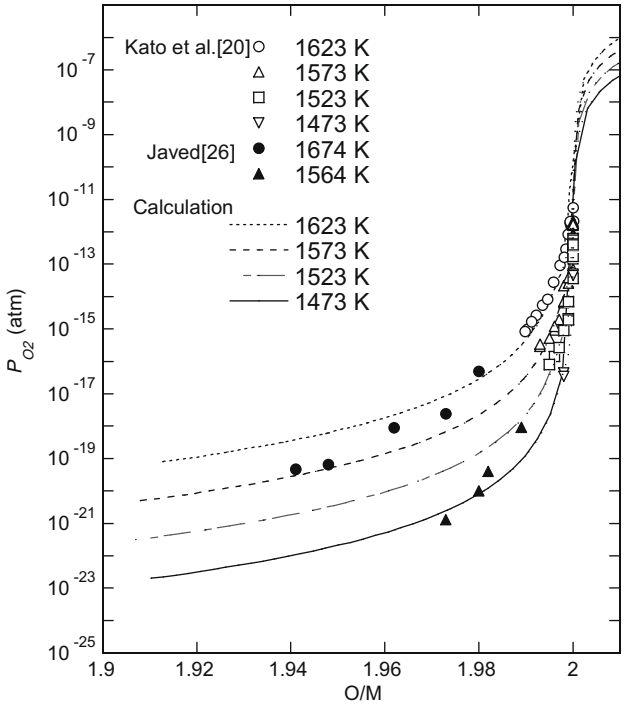

Fig. 8. Oxygen non-stoichiometry in $(U_{0.8}Pu_{0.2})O_{2\pm x}$ as a function of temperature and P_{O_2}.

agreement with the data of Kato et al. [20], and $\Delta\bar{H}_{O_2}$ and $\Delta\bar{S}_{O_2}$ of stoichiometric composition are obtained as $-674.0\ \mathrm{kJ\cdot mol^{-1}}$ and $-219.4\ \mathrm{J\cdot mol^{-1}}$, respectively; these are lower than the corresponding values of $(U_{0.7}Pu_{0.3})O_{2\pm x}$. The calculation curves did not represent the data of Javed [26]. His data were measured by gas equilibration and chemical analysis which has greater error as compared with the thermal gravimetry. It is considered that experimental data with precision are needed in hyper- and hypo-stoichiometric MOX containing 20% Pu.

4. Conclusion

The oxygen partial pressure of non-stoichiometric MOX was studied based on defect chemistry. The equilibrium constants of each reaction containing the defects were estimated by measured data of oxygen potential. The concentrations of each defect were estimated by the equilibrium constants. The following conclusions were obtained.

(1) The intrinsic ionization defect was dominant in near stoichiometric MOX.
(2) The dominant types of defects depended on the Pu content for the hypo-stoichiometric MOX. The $(2V_O^{\cdot\cdot}2Pu')^{\cdot}$ was the major defect species for $(U_{0.7}Pu_{0.3})O_{2-x}$ and $(V_O^{\cdot\cdot}Pu')^{\cdot}$ was for $(U_{0.8}Pu_{0.2})O_{2-x}$. This difference may be explained by the difference in the number of Pu ions which occupy the first neighbor site of an oxygen vacancy.
(3) The values of thermodynamic properties were estimated as follows: $\Delta\bar{H}_{O_2} = -552.5\ \mathrm{kJ\cdot mol^{-1}}$ and $\Delta\bar{S}_{O_2} = -149.7\ \mathrm{J\cdot mol^{-1}}$ for $(U_{0.7}Pu_{0.3})O_{2.00}$; $\Delta\bar{H}_{O_2} = -674.0\ \mathrm{kJ\cdot mol^{-1}}$ and $\Delta\bar{S}_{O_2} = -219.4\ \mathrm{J\cdot mol^{-1}}$ for $(U_{0.8}Pu_{0.2})O_{2.00}$.

References

[1] M. Katsuragawa, H. Kashihara, M. Akebi, J. Nucl. Mater. 204 (1993) 14–22.
[2] K. Asakura, T. Yamaguchi, T. Ohtani, J. Nucl. Mater. 357 (2006) 126–137.

[3] C. Sari, U. Benedict, H. Blank, J. Nucl. Mater. 35 (1970) 267–277.
[4] T.L. Markin, R.S. Street, J. Inorg. Nucl. Chem. 29 (1967) 2265–2280.
[5] J.J. Carbajo, G.L. Yoder, S.G. Popv, V.K. Ivanov, J. Nucl. Mater. 299 (2001) 181–198.
[6] K. Morimoto, M. Kato, M. Ogasawara, M. Kashimura, J. Nucl. Mater. 374 (2008) 378–385.
[7] M. Kato, H. Uno, T. Tamura, K. Morimoto, K. Konashi, Y. Kihara, Recent Advances in Actinide Science (2006) 367.
[8] Hj. Matzke, J. Nucl. Mater. 114 (1983) 121–135.
[9] P.E. Blackburn, J. Nucl. Mater. 46 (1973) 244–252.
[10] P.E. Blackburn, C.E. Johnson, IAEA-SM-190/50 (1974) 17–33.
[11] T.M. Besmann, T.B. Lindemer, J. Nucl. Mater. 130 (1985) 489–504.
[12] M. Stan, P. Cristea, J. Nucl. Mater. 344 (2005) 213–218.
[13] A. Nakamura, T. Fujino, J. Nucl. Mater. 167 (1989) 36–46.
[14] A. Nakamura, T. Fujino, J. Nucl. Mater. 140 (1986) 113–130.
[15] P. Karen, J. Solid, State Chem. 179 (2006) 3167–3183.
[16] K. Sasaki, J. Maeir, J. Appl. Phys. 86 (10) (1999) 5422–5433.
[17] P. Kofstad, Nonstoichiometry, Diffusion and Electrical Conductivity in Binary Metal Oxides, John Wiley and Sons, New York, 1972.
[18] O.T. Sørensen, Nonstoichiometric Oxides, Academic Press, New York, 1981. 1–59.
[19] M. Kato, T. Tamura, K. Konashi, S. Aono, J. Nucl. Mater. 344 (2005) 235–239.
[20] M. Kato, T. Tamura, K. Konashi, J. Nucl. Mater. 389 (2009) 89.
[21] P.R. Vasudeva Rao, S. Anthonysamy, M.V. Krishnaiah, V. Chandramouli, J. Nucl. Mater. 348 (2006) 329–334.
[22] T.L. Markin, E.J. McIver, Plutonium 1965, Chapman and Hall, London, 1967. 845-857.
[23] The Plutonium–Oxygen and Uranium–Plutonium–Oxygen Systems: A Thermochemical Assessment, Tech. Report Ser. No.79, IAEA, Vienna, 1967, pp. 52–66.
[24] G. R. Chilton, J. Edwards, United Kingdom Atomic Energy Authority Northern Division Report, ND-R-276(W), 1980.
[25] G.R. Chilton, I.A. Kirkham, Plutonium 1975 (1976) 171–180.
[26] N.A. Javed, J. Nucl. Mater. 47 (1973) 336–344.
[27] G. Brouwer, Philips Res. Rep. 9 (1954) 366–376.
[28] F.A. Kröger, H. Vink, Solid State Phys. 3 (1956) 307.
[29] F. Schmitz, A. Marajofsky, IAEA-SM-190/22 (1974) 457–468.
[30] F. Schmitz, J. Nucl. Mater. 58 (1975) 357–360.
[31] L. Manes, B. Manes-Pozzi, Plutonium and Other Actinides 1975 (1976) 145.
[32] M. Beauvy, J. Nucl. Mater. 188 (1992) 232–238.
[33] B.T.M. Willis, J. Chem. Soc. Faraday Trans. 2 (1987) 83.
[34] K. Naito, T. Tsuji, T. Fujino, T. Yamashita, J. Nucl. Mater. 169 (1989) 329–335.
[35] T. Fujino, T. Yamashita, K. Ohuchi, K. Naito, T. Tsuji, J. Nucl. Mater. 202 (1993) 154–162.